The Impact of subicular VIP-expressing interneurons on seizure dynamics in temporal lobe epilepsy: Insights from preclinical models

Sadegh Rahimi[1], Pariya Salami[2], Pawel Matulewicz[1], Armin Schmuck[1], Anneliese Bukovac[1], Ramon Tasan[1], Meinrad Drexel[1*]

1 Department of Pharmacology, Medical University of Innsbruck, Austria

2 Department of Neurology, Massachusetts General Hospital and Harvard Medical School, Boston, MA, USA

* Corresponding author:

meinrad.drexel@i-med.ac.at

Abstract

Temporal lobe epilepsy (TLE) is a high burden neurological disorder, affecting millions of individuals worldwide. Despite extensive research, the exact mechanisms underlying TLE remain unknown. It has been suggested by recent studies that the subiculum may serve as a hub for seizure generalization in TLE. The need for studying subicular vasoactive intestinal polypeptide expressing interneurons (VIP-INs) has been highlighted in the literature; however, the role of subicular VIP-INs in TLE has not yet been studied. The aim of the current study is to assess the possible role of subicular VIP-INs in the pathophysiology of TLE and its interaction with circadian rhythm.

We permanently inhibited neurotransmitter release selectively from VIP-INs of the ventral subiculum by injecting a viral vector expressing tetanus toxin light chain (AAV-TeLC) in epileptic as well as non-epileptic VIP-cre mice. Mice were then subjected to telemetric EEG recording for up to 50 days. In a subset of animals, the effect of bilateral injection of AAV-TeLC was assessed using local field potential recording. Furthermore, the possibility of manipulating seizures via stimulation of VIP-INs was explored by injecting a vector expressing GqDREADD.

In non-epileptic mice, injection of AAV-TeLC and AAV-GFP did not cause development of seizures in both groups. No change in vigilance states was observed. In epileptic animals, a significant reduction was observed in the average number of spontaneous seizures per day as well as the average time spent in seizure per day in AAV-TeLC-injected mice compared to AAV-GFP-injected controls, which was more prominent during the light phase. Interestingly, stimulation of VIP-INs had a significant proconvulsive effect.

In conclusion, our study provides the first evidence for the involvement of subicular VIP-INs in the pathogenesis of TLE. Further research using techniques such as cell type-specific electrophysiology and *in vivo* imaging will enhance our understanding of subicular VIP-INs in the context of epilepsy and pave the way for the development of gene-targeted cell type-specific therapies.

Introduction

Accumulating evidence from both clinical and experimental studies has shed light on the molecular changes, hypersynchrony, and abnormal anatomical structure of the subiculum underlying epileptic seizures (1). A spontaneous, rhythmic activity, initiated exclusively in the subiculum, was observed in brain slices of patients with temporal lobe epilepsy (TLE) more than two decades ago. These synchronous events were similar to interictal discharges of patients' electroencephalograms (EEG)(2). By examining resected hippocampi obtained from individuals with TLE, it was observed that there were no variations in the spontaneous epileptiform activities in the subiculum between sclerotic and nonsclerotic tissues (3). This suggested that modifications in synaptic transmission and intrinsic properties of the subiculum are crucial to the development of epilepsy, rather than deafferentation alterations. In line with the clinical findings that the subiculum remains relatively intact in TLE (4), animal experiments also indicated that subiculum neuron loss was significantly less detectable than that in the CA1/ CA3 regions (5). The subiculum primarily consists of glutamatergic pyramidal neurons, which show alterations in intrinsic excitability in the course of epilepsy (6–8), and multiple types of GABAergic interneurons, which exhibit varying characteristics in epilepsy.

The estimated proportion of GABAergic interneurons in the hippocampus is merely 10% to 15% of the total neuronal population (9); nevertheless, due to their vast anatomical and physiological diversity, these interneurons are capable of exerting a significant regulatory influence on almost all aspects of cellular and circuit functions (10). The dysfunction of subicular interneurons in epilepsy can be simplified as an imbalance of excitation and inhibition (E/I); however, interneurons are interconnected in numerous complex circuit patterns, including feedforward, feedback, and disinhibitory interconnectivity (11). Therefore, the three largest subclasses of subicular interneurons, which express parvalbumin (PV-INs), somatostatin (SST-INs), or vasocactive intestinal peptide (VIP-INs), may play opposing roles in TLE pathophysiology. PV-INs interneurons of the subiculum and CA1 selectively degenerate in animal models of TLE (12, 13). Moreover, selective silencing of PV-containing basket cells and axo-axonic cells of the subiculum, by decreasing the perisomatic inhibition of pyramical cells, resulted in recurrent series of interictal spikes and spontaneously recurrent seizures in more than 60 percent of the animals (14). Loss of SST-INs in the CA1 region of the hippocampus following pilocarpine-induced seizures was also reported (15). In addition, decreased dendritic inhibition of pyramical cells by permanent functional silencing of subicular SST-INs caused spontaneous seizures in almost one-third of animals (16). Changes in the numbers and properties of subicular PV-INs and SST-INs in epilepsy were well described (1). Although VIP-INs are relatively sparse in comparison to PV-INs and SST-INs, their unique connectivity suggests they might be the principal players in the subicular circuit; however, their function in epilepsy remains unclear.

The hippocampal VIP-INs can be divided into two major groups based on their targets. The first group includes VIP- basket cells (VIP-BC), which are responsible for inhibiting the somatic region of pyramidal cells (PCs), are also immunoreactive for cholecystokinin (CCK). The second group consists of interneuron selective interneurons (IS INs) that selectively innervate other interneurons. There are two subtypes of IS INs: (a) interneurons with cell bodies located at the stratum pyramidale (SP) or near and projecting to the stratum Oriens/Alveus border (VIP-IS O/A INs or IS cells type III), co-expressing calretinin (CR), mostly target SST-expressing oriens lacunosum-moleculare (OLM) interneurons, and (b) VIP-INs that project their axons to the stratum radiatum (SR), with cell bodies located either at the SR/ stratum lacunosum-moleculare border (IS cells type II) or at SR/SP, targeting interneurons controlling synaptic transmission to proximal dendrites of SR's PCs (17–19). In human TLE, the loss of pyramidal neurons was linked to the upregulation of VIP receptors in the hippocampus; however, the distribution and pattern of VIP-INs remained unaltered (20). Children suffering from chronic epilepsy displayed higher levels of VIP in their cerebrospinal fluid (21). Additionally, in focal cortical dysplasia (type IIb), the primary cause of medically intractable pediatric epilepsy, there was a notable increase in the ratio of VIP-INs to other interneurons (22). In rodent, increased firing rates of VIP-INs were observed in tubocurarine-treated cortical slices as spikes and waves developed (23). Interestingly, most VIP-INs are preserved also in animal model of epilepsy (24, 25), although the OLM interneurons, which are targeted by VIP-INs, are selectively lost (26). Although there is increasing evidence indicating the potential significance of VIP-INs in TLE, there is a lack of consensus in the interpretation of their role. The upregulation or lack of change in VIP-INs expression can be interpreted as either causative (22, 24) or compensatory (27) in the context of epileptic excitotoxicity. Additionally, no studies have explored the functional role of VIP-INs in the subiculum. While subicular IS type II and III disinhibit pyramidal cells, VIP-BCs innervate directly innervate PCs. The collective effect of these subgroups in the epileptic brain remain unexplored, which may have significant implications for the overall understanding of their function in TLE.

In order to investigate the potential involvement of subicular VIP-INs in TLE, we selectively blocked the release of neurotransmitters from these neurons in the subiculum of mice, and continuously monitored their EEG using telemetric recording. We conducted this experiment both in non-epileptic mice, as well as in mice with chronic epilepsy, in order to evaluate the potential role of VIP-INs in a compromised network architecture. In addition, we expressed hM3Dq receptors specifically in VIP-INs and utilized this to transiently stimulate GABA release from these neurons by administering clozapine N-oxide (CNO) in an acute seizure model. Our findings suggest that silencing VIP-INs in the ventral CA1/subiculum of healthy controls does not elicit epileptiform activity. However, in epileptic mice, silencing of VIP-INs reduces the severity of seizures. Intriguingly, activation of VIP-INs in mice in a model of acute seizures increases epileptiform activity. Our findings are consistent with the

disinhibitory function of VIP-INs in the cortex and underscore the predominant contribution of subicular IS type II and III, compared to subicular VIP-BC, in both epileptic and non-epileptic states.

Result

Silencing of VIP-INs in ventral CA1/subiculum of healthy mice does not induce seizure or epileptiform activity

Telemetric EEG recordings were conducted for continuously 50 days in male VIP-Cre mice injected unilaterally with AAV-TeLC (n=5) or AAV-GFP (n=5) into the ventral subiculum (Fig 1A). The recorded EEG were visually reviewed (see Methods) and no seizures were detected in any of the AAV-TeLC- or AAV-GFP-injected animals (Fig 1B). To evaluate the precision of vector targeting, at the end of the study, the specificity of the vector in targeting VIP-INs was investigated. Quantitative assessment was performed on four AAV-TeLC- and four AAV-GFP-injected animals. In addition to subiculum, variable expression of TeLC (fused with GFP) was also detected in the sector CA1, presubiculum, and parasubiculum and occasionally in parts of the entorhinal cortex. At the injection site, 46.67% (41.18% to 90%) of the VIP-INs expressed GFP, while 95.84% (82.35% to 100%) of the GFP-expressing interneurons also co-expressed VIP (Fig 1C), highlighting the specificity of the experimental manipulation using the TeLC vector.

To avoid missing subtle focal epileptiform activity, we repeated the experiment by bilateral injection of AAV-TeLC (n=4) or AAV-GFP (n=4) into the ventral subiculum (S1 Fig). Recordings were performed for 21 days and data were reviewed visually. No seizures were detected in either group. Epileptiform spikes (Fig S1) and spike trains were also assessed for three consecutive days, 6 hours per day (from 18:00 to 24:00, starting from day 18). We observed a negligible number of epileptiform spikes and spike trains. The median (range) cumulative number of epileptiform spikes was 148 (3 to 1687) and 1500 (24 to 4723) for GFP and TeLC animals, respectively (S1 Fig). There was no significant difference between the groups. The median (range) number of spike trains was 0.0 (0.0 to 37) and 13.50 (0.0 to 31) for GFP and TeLC animals, respectively (S1 Fig), and there was no significant difference between the groups.

Silencing VIP-INs in epileptic mice dampens seizures

The lack of epileptic activity resulting from the silencing of subicular VIP-INs may be attributed to their disinhibitory role, or simply due to the very low number of these cells in the ventral subiculum. To rule out the latter possibility, we silenced subicular VIP-INs in a chronic model of epilepsy by intrahippocampal kainic acid (IH-KA) injection. The telemetric EEG transmitters were implanted in 16 VIP-Cre mice (8 females), who also received IH-KA injections on the same day (Fig 2A). The animals

were blindly divided into two groups, to later receive either AAV-GFP or AAV-TeLC after 7 days. Before administering the vector injection, the severity of status epilepticus (SE) and subsequent spontaneous recurrent seizures were evaluated to establish the baseline epileptic activity of both groups. During SE (day 1), the median (range) number of seizures was 10 (1 to 19) and 8.5 (1 to 14) for the GFP and TeLC groups, respectively (Fig 2C). The median (range) cumulative duration of seizures was 314.1 s (10.34 s to 1098 s) for the GFP group and 266.10 s (17 s to 703 s) for the TeLC group (Fig 2I). No significant difference was observed between the groups based on the number or time spent in seizures during SE. As seizure during SE does not always reveal postictal depression (S2B Fig), the number of seizures may be underestimated. Therefore, we also compared the groups based on the number of epileptiform spikes and spike trains. During SE, the median (range) number of epileptiform spikes in the GFP group was 54511 (32651 to 153106) and 68674 (33018 to 153892) for TeLC mice (S2D Fig). No significant difference was observed between the groups. The median (range) number of spike trains was 3519 (1993 to 18226) for the GFP group and 6439 (1996 to 15306) for the TeLC group (S2F Fig). No difference was observed between the groups.

Recordings were reviewed during the six days of recording after SE but before vector injection. The median (range) number of seizures (SRSs) was 1.50 (1 to 12) and 4.50 (2 to 13) for the GFP and TeLC groups, respectively (Fig 2D and Fig 2F), showing no significant difference between the groups. The vectors were injected on Day 7, and after a two-week waiting period, the number and duration of seizures was assessed and compared between the groups. While the median (range) number of seizures increased in the GFP group to 7 (0 to 14), the value decreased for the TeLC group to 3 (0 to 7), showing a significant difference between two groups ($p < 0.05$, Fig 2E-F). Considering the individual differences in the number of seizures in the IH-KA model, we also assessed the seizure ratio for each animal by comparing the number of seizures before and after vector injection (Fig 2G). The median (range) seizure ratio was 0.55 (-1.00 to 0.86) for the GFP group and -0.33 (-1.00 to 0.42) for the TeLC group. The GFP mice generally showed an increasing trend in the number of seizures, while the ratio was decreasing for the TeLC group, with a significant difference ($p < 0.05$) between groups. The circadian changes in the seizure ratio in both groups were further assessed (S3 Fig) and found to have a significant reduction during the light phase ($p < 0.05$), while the reduction was not significant during the dark phase (Fig 2 H).

In addition to comparing the number of seizures, we also evaluated the groups based on the duration of seizures. The median (range) time spent in seizure (cumulative duration) prior to vector injection was 48.81 s (10 s to 517 s) for GFP mice and 168.8 s (87.36 s to 210.70 s) for TeLC mice, respectively (Fig 2J and 2L). No significant difference was detected between the groups. Following vector injection, the median (range) cumulative duration of seizures increased to 285.4 s (0 to 499.4 s) for the GFP

group, while it decreased to 85.15 s (0.0 to 264.4 s) for the TeLC group (Fig 2K-L). A significant difference was observed between the groups ($p < 0.05$). We also assessed the seizure duration ratio for each animal, finding a median (range) of 0.66 (-1.0 to 0.96) for GFP mice and -0.36 (-1.0 to 0.34) for TeLC mice, indicating a significant difference ($p < 0.05$, Fig 2M). The reduction in time spent in seizures was more prominent during the light phase ($p < 0.05$, Fig 2N), similar to the trend observed for the number of seizures.

Furthermore, we evaluated the rate of high-frequency oscillations (HFOs) and more specifically that of fast ripples (FRs) as an additional measure for disease severity. Individual FRs were initially detected using automated methods and were then visually validated in two 10 minutes periods during light and dark phases in each animal over Day 2 to Day 7 and again over Day 22 to Day 27 (like seizures). The rate of occurrence, average duration and average amplitude of isolated FRs were then compared between the groups (S4 Fig). Since the incidence of isolated FRs has not been reported in the early stage of the IH-KA model in mice, the potential of the model to generate isolated FRs was assessed during the first six days after KA injection (prior to vector injection). Interestingly, isolated FRs were observed in all animals on the immediate day after SE during both the light and dark phases. The median (range) number of isolated FRs per 10-minute bin in the GFP group was 3.08 (0.83 to 14.50) during the light phase and 2.5 (0.33 to 10.3) during the dark phase. The corresponding measure in the TeLC group was 2.25 (0.50 to 8) during the light phase and 2.16 (0.16 to 6.20) during the dark phase (S4C and S4F Fig). No significant difference was found between the two groups during the light and dark phases (S4C and S4F Fig, S1 Table). The incidence of isolated FR was evaluated again two weeks after vector injection. During the light phase, the median (range) number of isolated FR in each 10-minute bin was 2.41 (0.0 to 5.33) for the GFP group and 1.58 (0.33 to 17.83) for the TeLC group. During the dark phase, the median (range) number of isolated FR in each 10-minute bin was 0.5 (0.0 to 10.83) for the GFP group and 0.75 (0.0 to 12.83) for the TeLC group (S4C and S4F Fig). No significant difference was observed in the number of isolated FRs between groups after vector injection, and the incident ratio of isolated FRs also showed no significant difference between groups (S4C and S4F Fig, S1 Table). Additionally, no significant differences were found between groups in the average duration and amplitude of isolated FRs during the light and dark phases before and after vector injection (S4D-E and S4G-H Fig, S1 Table).

Activating VIP-INs in epileptic mice increases seizures

If silencing subicular VIP-INs decreases seizures in the chronic model of epilepsy, activation of them should increase seizure. To test this hypothesis, AAV-hM3D(Gq) was injected into 15 VIP-Cre mice (5 female), and the acute seizure model was achieved by IH-KA injection on day 10 (Fig 3A). The animals

were blindly divided into two groups, CNO (n=9) or NaCl (n=6), and administered an i.p. injection of CNO or NaCl half an hour before the IH-KA injection. All animals developed seizures within the first hour after IH-KA injection (Fig 4B). The median (range) number of seizures in the NaCl group was 2 (1 to 4), while the value was 5 (2 to 7) for the CNO group. A significant difference was observed between the groups ($p < 0.05$). The median (range) cumulative duration of seizures for the NaCl group was 76.02 s (33.08 s to 150.50 s) and 138.70 s (51.89 s to 225.0 s) for the CNO group. Although a strong trend was observed, no significant difference was found between the groups.

Discussion

Our results provide new insights into the pivotal role of VIP-INs in controlling the excitability of PCs in the subiculum in context of epilepsy. In line with our expectations, permanent unilateral or bilateral silencing of subicular VIP-INs in non-epileptic animals did not induce seizure or epileptiform activity. Despite the heterogeneity of subicular VIP-INs and the lower number of VIP-INs compared to PV-INs and SOM-INs (14, 16), anatomically restricted inhibition of subicular VIP-INs, with 95% specificity, was sufficient to reduce seizures in the chronic model of epilepsy, emphasizing the critical role of this small cell population in modulating TLE. Intriguingly, even transient activation of VIP-INs in the subiculum was enough to increase the frequency of seizures in the acute seizure model (Fig 4).

Subicular VIP-INs comprise two main subtypes, VIP-BCs and IS type II and III (ISs), with opposing roles in the subicular network. While VIP-BCs directly innervate PCs, ISs disinhibit PCs. Our findings in both healthy and epileptic animals indicate a more dominant role for ISs. To our knowledge, no previous study has investigated the specific role of subicular VIP-INs in the pathogenesis of TLE. However, a limited number of studies have examined both VIP-BCs and ISs in hippocampal sector CA1 in different animal models of epilepsy. In the IH-KA model, it was reported that the number of CCK-INs (of which VIP-BCs constitute almost 27% (9)) was reduced in the ventral hippocampi after KA injection, although the surviving CCK-BCs did not exhibit significant changes in their intrinsic and synaptic properties or connectivity with CA1 PCs (28). In the pilocarpine model of epilepsy in mice, the overall density of IS type III interneurons remained preserved (26, 25), but the number of axonal boutons produced by these cells within the CA1 O/A was significantly lower after SE (26). In addition, VIP+/CR- INs, which contain both IS type II and VIP-BCs, decreased to 54% compared to non-epileptic animals (25). No study has evaluated the vulnerability of IS type II cells specifically in the context of epilepsy. It might be argued, that VIP-BCs are more susceptible to damage than ISs in the IH-KA model of epilepsy. As a result, the balance of cell types may shift, leading to a greater impact from ISs when VIP-INs are silenced in the chronic model of epilepsy; however, the results of silencing VIP-INs in non-epileptic

animals and in the acute model of seizure, in which these cells were activated 30 minutes prior to IH-KA injection, support the predominant role of ISs regardless of the number of viable cells.

VIP is exclusively expressed by GABAergic interneurons in hippocampus (29); however, the prominent observed role of subicular VIP-INs in TLE can be modulated not only by GABA release from these interneurons, but also by endogenous VIP. VIP interacts with two receptors, VPAC1 and VPAC2, as well as PAC1 with lower affinity (27). VPAC1, VPAC2 and PAC1 receptors stimulate the cAMP/PKA signaling pathway and are positively coupled to $G_{\alpha s}$ (30). In the hippocampus, VPAC1 receptors can also couple to $G_{i/o}$ proteins (31). Although no study has yet identified VPAC1 receptors in hippocampal interneurons, their inhibition of OLM cells suggests that VPAC1 receptors are expressed there (for more review please read (32)). VPAC2 receptors are the primary mediators of VIP enhancement of PCs excitability and NMDA receptor currents, effects that are mainly post-synaptic and independent of GABAergic transmission (33). In human hippocampi surgically removed from patients with medically intractable TLE, a significant upregulation of VIP receptors on PCs was observed (20), indicating an increased excitation of these cells by VIP. In vitro, the selective VPAC1 antagonist PG 97-269 has been shown to contribute to the inhibition of LTP that follows interictal-like activity in hippocampal slices (34). Furthermore, a recent study observed a compensatory decrease in VPAC1 receptor levels in mice Lithium-pilocarpine models, while VPAC2 receptor levels are increased in hippocampal membranes (35), highlighting the critical role of VIP and its receptors in the pathophysiology of TLE.

We have reported the occurrence of HFOs and more specifically fast ripples in our recordings. Although there has been growing interest in HFOs in human epilepsy and several animal models of epilepsy in recent years, HFOs have not been well characterized in mouse models of IH-KA epilepsy. Recently it was shown that much like human and other models of epilepsy, HFOs may be recorded from the epileptogenic regions and other areas of this mouse model of epilepsy (36). An important limitation of our study is that we only recorded from the somatosensory cortex of the animals. In addition to pathological HFOs, this region may also give rise to physiological HFOs (37). Therefore, the presence of HFOs in our study may suggest a wider network involvement in the epileptogenicity but they may also be of physiological origin. Given that we have seen HFOs but did not find any significant differences between the two groups, more experiments involving recordings from additional regions need to be performed to conclusively distinguish between physiological and pathological HFOs.

There were some limitations to this study that need to be considered. While our injection of TeLC was highly specific (over 90%), we were unable to target all VIP-INs in the subiculum, reflected by the sensitivity of about 60%. Additionally, we observed variable expression of TeLC in other brain regions, including sector CA1, presubiculum, parasubiculum, and occasionally in parts of the entorhinal cortex.

To optimize our targeting, before starting the main experiments, we tried several different doses and selected the best options. However, future studies that use new technologies may enable more precise targeting of the subiculum and its interneurons, including VIP-INs. Another limitation was the high variation in the number of seizures observed among animals in the chronic model of epilepsy, which was expected (38). To ensure the robustness of our findings, we reported the number (and duration) of seizures also as a ratio for each animal compared to the number (and duration) of seizures before injection. It is important to note that evaluating the same question in different animal models of epilepsy may provide further insight.

In conclusion, our study provides the first evidence for the involvement of subicular VIP-INs in the pathogenesis of TLE. Given the predominant disinhibitory role of the VIP-INs input in subicular microcircuits, modifications of this input may be considered in the development of therapeutic strategies to improve seizure control. Further research using techniques such as cell type-specific electrophysiology and *in vivo* imaging will enhance our understanding of subicular VIP-INs in the context of epilepsy and pave the way for the development of gene-targeted cell type-specific therapies.

Method

Mice

The experiments involving animals were carried out in compliance with national regulations and European Community laws, and were granted approval by the Committee for Animal Protection of the Austrian Ministry of Science. The VIP-cre transgenic mice (Vip$^{tm1(cre)Zjh}$/J, RRID:IMSR_JAX:010908) , which express Cre-recombinase under the VIP promoter and were initially obtained from The Jackson Laboratory through Charles River, were maintained on a C57BL/6N background. C57BL/6N wild-type (WT) mice were acquired from Charles River. The mice were kept in groups of 3 to 5 in ventilated cages and provided with food and water *ad libitum* under standard laboratory conditions (12-hour light/dark cycle, with lights on at 7:00 A.M.). The experiments were conducted using male and female heterozygous mice aged 10 to 14 weeks.

Preparation of the vectors

The AAV2/6 vectors carried either tetanus toxin light chain (TeLC) fused with a GFP tag or GFP alone, with their reading frames inverted in a FLEX cassette (AAV-TeLC and AAV-GFP, respectively). Thus, AAV-mediated transgene expression is limited to VIP-INs at the injection site (39). Vectors pseudotyped for AAV2/6 were produced and purified as previously described (40). Briefly, HEK293 cells were

cotransfected with rAAV plasmids pAM-FLEX-TeLC or pAM-FLEX-GFP and pDP1rs helper plasmids by calcium phosphate coprecipitation. Benzonase-treated cleared cell lysates were purified by HPLC on AVB columns with successive dialysis. The AAV titers were quantified by PCR as the number of genomic particles per milliliter (gp/ml), with titers of 1 × 1012 gp/ml for pAM -FLEX-TeLC and 1 × 1013 gp/ml for pAM -FLEX-GFP. To ensure that TeLC was fully active, we evaluated all seizure-related factors after 14 days of the injection. As already noted, the silencing will remain permanent afterward (39).

For experiments using DREADD technology, rAAV6-hSyn-DIO-hM3D(Gq)-mCherry (Addgene 44361) was kindly provided by B. Roth, obtained from Addgene (USA) and packaged in our laboratory as described in detail previously (41). It was packaged into AAV2 capsids and was injected with a final titer of 9×10^{12} gp/ml.

Surgery

Stereotaxic surgeries were performed as described in detail previously (14). Heterozygous male and female VIP-cre transgenic mice (age, 10–14 weeks) were treated with the analgesic drug meloxicam (5 mg/kg, s.c.) 15 min before surgery. They were anesthetized with 150 mg/kg, i.p. ketamine (stock solution 50 mg/ml; Ketasol, Ogris Pharma Vertriebs-GmbH, Wels, Austria) and anesthesia was maintained by applying 1–3% sevoflurane (3% for induction, 1–1.5% for maintenance; Sevorane, Abbott, IL, USA) through a veterinary anesthesia mask using oxygen (400 ml/min) as a carrier gas. Mice were mounted into a stereotaxic frame (David Kopf Instruments) and the skin above the skull was opened. We then placed a telemetry EEG transmitter (ETA-F10, Data Sciences International, St. Paul, MN, USA) into a subcutaneous pocket on the left abdominal wall, and the two connected electrode wires were pulled through the subcutaneous channel (between the pocket and exposed skull); the pocket was carefully sutured afterward. Bilateral holes were drilled for AAV vector injection, insertion of an epidural recording electrode (coordinates from bregma: posterior, 2.0 mm, lateral, 1.6 mm) and for an epidural reference electrode (coordinates from bregma: posterior, 2.0 mm, lateral, -1.6 mm). In a subset of the animals, for the detection of focal epileptiform activity, we recorded local field potentials (LFP). In those animals, the depth electrode (coordinates from bregma: 1.9 mm posterior, 1.6 mm, lateral, 1.9 mm ventral) was inserted above ipsilateral CA1 instead of the epidural recording electrode. Electrodes were fixed to the skull using dental cement (Paladur, Heraeus Kulzer supplied by Henry Schein, Innsbruck, Austria). We then injected 1 µL of AAV-TeLC or AAV-GFP at a rate of 0.1 µl/min unilaterally into the transition zone of the left ventral subiculum and sector CA1 (coordinates from bregma: 3.6 mm posterior, 3.2 mm lateral, 3.6 mm ventral). After injection, the cannula was left in place for 10 minutes before it was slowly retracted. In order to increase the effect of silencing of subicular VIP-INs in the subiculum, in mice that underwent depth electrode recording, AAV-TeLC or

AAV-GFP was injected bilaterally, with the same coordinates as the unilateral injection (3.6 mm posterior, ± 3.2 mm lateral, 3.6 mm ventral). The AAV-TeLC or AAV-GFP injections were done on the same days in mice of the same litters. After surgery, the mice were single housed.

To achieve specific and reversible chemogenetic activation of VIP-INs in the subiculum, we used DREADD technology. Male and female heterozygous VIP-cre mice were injected with rAAV6-hSyn-DIO-hM3D(Gq), 0.5 µL, at a rate of 0.1 µL/min into the left ventral subiculum using the same coordinates and protocol as for AAV-TeLC injections.

Induction of the chronic model of epilepsy by intrahippocampal kainic acid (IH-KA) injection

During transmitter implantation surgery of male and female heterozygous VIP-cre mice, KA was intrahippocampally injected (200 ng in 140 nL phosphate-buffered saline [PBS], pH 7.4, injection speed 140 nL/min; pump: Ascent Scientific, North Somerset, UK) to test the possible outcome of silencing VIP-INs in epileptic animals. The injection cannula (polyimide-coated silica capillary tubing: 150 µm outer diameter; TSP075150, Polymicro Technologies) was attached to a 1 µL Hamilton syringe using fine-bore polythene tubing (800/100/100; Smiths Medical International, Kent, UK) and connected to a precision syringe pump (Nexus 3000 by Chemyx, Science Products, Hofheim, Germany). Following the injection, the cannula remained in place for 3 minutes before being slowly retracted. EEG recording was then recorded immediately as the mice were transferred to their cages. All mice in the study experienced acute seizures after KA injection, and EEG activity returned to baseline after nearly 24 hours, which was considered as status epilepticus (SE) in the study. As an exclusion criterion, mice that did not develop spontaneous recurrent seizures (SRSs) before vector injection were excluded from the study.

Experimental model of acute focal seizures induced by injection of IH-KA

Ten days after injection of AAV- hM3Dq vector in male and female heterozygous VIP-cre mice, they were anesthetized briefly with 3% sevoflurane and injected intrahippocampally with KA (7 ng in 500 nL phosphate-buffered saline [PBS], pH 7.4, injection speed 500 nL/min; pump: Ascent Scientific, North Somerset, UK). The injection cannula (polyimide-coated silica capillary tubing: 150 µm outer diameter; TSP075150, Polymicro Technologies) was attached to a 1 µL Hamilton syringe using fine-bore polythene tubing (800/100/100; Smiths Medical International, Kent, UK) and connected to a precision syringe pump (Nexus 3000 by Chemyx, Science Products, Hofheim, Germany). After injection, the cannula was left in place for 1 minute before it was slowly retracted, and the mice were quickly transferred to their cages for EEG recording. Under these conditions, KA induced acute seizures in 100% of mice and EEG activity returned to baseline after 1-2 hours.

Transient activation of VIP-INs using the DREADD system

Seven days after AAV- hM3Dq injection, the transmitter was inserted in male and female heterozygous VIP-cre mice and telemetry EEG was recorded continuously until the end of the study. Three days later (day 10 after vector injection), the selective hM3Dq agonist clozapine-N-oxide (CNO, Tocris Bioscience; 5 mg/kg, i.p., dissolved in sterile 0.9% NaCl at a concentration of 1.0 mg/ml) was intraperitoneally injected. The control group of mice that received the AAV-hM3Dq vector injection were injected with saline instead of CNO. Thirty minutes after CNO injection, acute focal-onset seizures were induced by IH-KA injection, and the possible effects of activating VIP-INs on the number and duration of the seizures were evaluated via telemetry EEG.

EEG and LFP recording

Continuous EEG and LFP recordings were obtained using a telemetry system and Ponemah analysis software version 6.0.x. (Data Sciences International, St. Paul, MN, USA). To further analyze behavior, a cohort of animals underwent continuous video recordings during the dark phase, which were captured using Axis 221 network cameras (Axis Communications) and infrared illumination (Conrad Electronics). The EEGs and LFPs were recorded at a sampling rate of 1000 Hz and saved onto external hard disk drives, without any pre-defined filter cutoff.

Analysis of epileptiform activity

Two independent observers visually examined EEG and LFP traces using the Ponemah analysis software version 6.0.x. (Data Sciences International, St. Paul, MN, USA). Seizures were identified as periods of uninterrupted activity with a minimum duration of 10 seconds and an amplitude at least twice that of the baseline, along with the presence of postictal depression (EEG signal below baseline amplitude). In our cohort database, using simultaneous video recording, this signal corresponded to seizure racine scale 3-5 (14).

In order to distinguish epileptiform spikes from normal baseline spikes or those caused by electrical or mechanical artifacts, we analyzed specific features of each spike, including its amplitude, duration, frequency, and inter-spike intervals. A custom-made program developed in MATLAB 2020b (Mathworks, Natick, MA, USA) automatically detected spikes and spike trains offline, based on threshold crossings. Briefly, movement artifacts were removed automatically and then, a blind reviewer adjusted the threshold for spike detection to compensate differences in individual signal amplitude, ranging from 4 to 6 standard deviations. Epileptiform interictal spikes were characterized as short (10 to 80 ms) high-amplitude discharges above the threshold, with a minimum peak distance

of 150 ms. Detected spikes were then visually confirmed. Spike trains were defined as three or more spikes with a frequency greater than 1 Hz and lasting at least 1 second (42). Since postictal depression is not always visible during SE, in addition to comparing the groups based on the number of seizures, the severity of SE was also compared based on the number of epileptiform spikes as well as spike trains (43).

Analysis of high-frequency oscillations (HFO)

For each animal, two 10-minute artifact free interictal periods during dark and light phases were selected on days Day 2 to Day 7 (before vector injection) and again on Day 22 to Day 27 (after vector injection) for analysis of HFOs (44, 45). The selected interictal periods were at least 1 h away from any detected seizures. We employed a semi-automated approach from HFOApp (46), which offers a graphical interface for selecting and applying various algorithms to detect HFOs. Short time energy (STE) was used, which was described before in the context of HFOs detection (47, 48). In brief, the EEG was band-pass filtered between 80-200 (ripples) and 250-500 Hz (fast ripples) using a finite impulse response digital filter and the root mean square (RMS) amplitude of the filtered signal was measured. Oscillatory events were detected in each frequency band if they showed at least four consecutive cycles and had an amplitude of 3 standard deviations above the mean (49). Detected HFOs were then visually evaluated on the EEG along with their time-frequency power plots and false events were rejected. An artifact was recognized by its absence of a clear and defined central frequency, resulting in a distorted blob-like appearance in the spectrogram with a persistent, strong spectral power in the time-frequency domain. HFOs associated with artifactual events, movement, or other sources of noise were excluded. Since ripples could also occur in a physiological context (50), any overlapping of ripple and fast ripple (FR) were excluded and only isolated FR was considered for the rest of the study. The number of FRs, their duration, amplitude, and average number of cycles in each FR event were calculated.

Double-labeling by immunofluorescence

At the end of the experiment (depending on the experiment, 4-8 weeks after the initial vector injection), mice were deeply anesthetized (killed) with thiopental (150 mg/kg) and perfused with 4% paraformaldehyde. The brains were removed, and 40-µm-thick horizontal sections were prepared for immunofluorescence study. Monoclonal rat anti-GFP (1:2000; catalog #04404-84, Nacalai Tesque, through GERBU Biotechnik; RRID:AB_10013361) and rabbit anti-VIP (1:500; catalog #20077, Immunostar, through ACRIS, RRID: AB_572270) were used as primary antibodies. The antibodies were characterized by the supplier or were validated by us in previous experiments (16). For the double labeling of GFP and VIP, the horizontal sections were incubated with 10% normal goat or horse serum

(catalog #26050088, Gibco, through Thermo Fischer) in Tris-HCl-buffered saline (TBS; 50 mm), pH 7.2, containing 0.4% Triton X-100 (TBS-Triton) for 90 min, followed by incubation with the respective primary antisera for 16 h at room temperature. After washing with TBS-Triton, a secondary reaction was performed by simultaneous incubation with a donkey direct-conjugated to Alexa Fluor 488 antibody (1:500; catalog #A-21208, Molecular Probes) for GFP and with a biotin-coupled goat anti-rabbit antibody (1:500; catalog #A-16027, Invitrogen) for VIP at room temperature for 120 min. The sections were washed with TBS, incubated for 100 minutes in streptavidin (1:100; catalog #SA 5649, Vektor). They were washed with TBS again and subsequently mounted on slides in gelatin, then covered with mounting media (86% glycerol and 2.5% DABCO in PBS).

To count the neurons co-expressing TeLC/GFP and VIP at the AAV vector injection site, microphotographs of 40-µm-thick horizontal double immunofluorescence-labeled sections (four sections per mouse, ten mice) were taken at 20× primary magnification using a fluorescence microscope (Imager.M1, Carl Zeiss). The images were imported into NIH ImageJ 1.51d (National Institutes of Health, Bethesda, MD, USA), and photographs of the individual channels were displayed side by side. The area evaluated was defined by the region containing GFP-positive neurons (directly affected by the vector injection). The numbers of single-labeled and double-labeled cells were determined manually.

Statistical Analyses

The statistical analyses were conducted using GraphPad Prism statistical software (version 9.1.1; GraphPad Software). To compare seizure-related factors before and after vector injection, a two-way repeated-measures ANOVA with Sidak's multiple-comparison post hoc test was performed. Given the significant variation in seizure numbers observed in the IH-KA model (38), in addition to the cumulative number and duration of seizures, we reported the seizure ratio for each animal. This involved comparing the number (or duration) of seizures in each individual animal before and after vector injection, as defined by the formula (seizure after - seizure before) divided by (seizure after + seizure before). The differences between two groups were compared using non-parametric (distribution-free) Mann–Whitney U test. The correlation between isolated FRs features and seizure severity was evaluated using the Pearson correlation test. A p-value of less than 0.05 was considered statistically significant. The graphs were generated using GraphPad Prism 9.1.1 and MATLAB 2020b.

Acknowledgements

Professor Lisa Topolnik, Laval University, Canada, is to be thanked for providing valuable insight into the hippocampal disinhibitory circuit and its possible relevance to the findings of the current experiment. We also want to thank Dr. Arnau Ramos Prats and Pradeepa Mohan for their fruitful discussions and knowledgeable suggestions regarding the statistics and representation of the results. The authors thanks Atea Shkodra for herexcellent technical assistance. The study was supported by the Austrian Science Fund (Project P 31777 to M.D.).

Data availability

The EEG recordings and all algorithms implemented in this work can be made available upon request by contacting the first author (Dr. Sadegh Rahimi, Medical University of Innsbruck, Austria, sadegh.rahimi@i-med.ac.at).

Author contributions

S.R. designed the experiments, established and performed all surgeries, EEG recordings and analyses, and wrote the manuscript

R.T. provided vectors for circuit manipulation

P.S. contributed to the analysis of HFO experiment, wrote a part of manuscript

P.M. contributed to the depth electrode recording

A.S. analyzed the interictal spikes and the circadian change in seizures

M.D. conceived and designed the experiments and made all proofs of the manuscript

Competing interests

The authors declare no competing interests.

References

1. Fei F, Wang X, Wang Y, Chen Z. Dissecting the role of subiculum in epilepsy: Research update and translational potential. Prog Neurobiol 2021; 201:102029.

2. Cohen I, Navarro V, Clemenceau S, Baulac M, Miles R. On the origin of interictal activity in human temporal lobe epilepsy in vitro. Science 2002; 298(5597):1418–21.

3. Wozny C, Knopp A, Lehmann T-N, Heinemann U, Behr J. The subiculum: a potential site of ictogenesis in human temporal lobe epilepsy. Epilepsia 2005; 46 Suppl 5:17–21.

4. Blümcke I, Thom M, Aronica E, Armstrong DD, Bartolomei F, Bernasconi A et al. International consensus classification of hippocampal sclerosis in temporal lobe epilepsy: a Task Force report from the ILAE Commission on Diagnostic Methods. Epilepsia 2013; 54(7):1315–29.

5. Drexel M, Preidt AP, Sperk G. Sequel of spontaneous seizures after kainic acid-induced status epilepticus and associated neuropathological changes in the subiculum and entorhinal cortex. Neuropharmacology 2012; 63(5):806–17. Available from: URL: https://www.sciencedirect.com/science/article/pii/s0028390812002675.

6. Chung S, Spruston N, Koh S. Age-dependent changes in intrinsic neuronal excitability in subiculum after status epilepticus. PLoS ONE 2015; 10(3):e0119411.

7. Fei F, Wang X, Xu C, Shi J, Gong Y, Cheng H et al. Discrete subicular circuits control generalization of hippocampal seizures. Nat Commun 2022; 13(1):5010.

8. Lippmann K, Klaft Z-J, Salar S, Hollnagel J-O, Valero M, Maslarova A. Status epilepticus induces chronic silencing of burster and dominance of regular firing neurons during sharp wave-ripples in the mouse subiculum. Neurobiol Dis 2022; 175:105929.

9. Bezaire MJ, Soltesz I. Quantitative assessment of CA1 local circuits: knowledge base for interneuron-pyramidal cell connectivity. Hippocampus 2013; 23(9):751–85.

10. Kenneth A. Pelkey, Ramesh Chittajallu, […], and Chris J. McBain. Hippocampal GABAergic Inhibitory Interneurons.

11. Kepecs A, Fishell G. Interneuron cell types are fit to function. Nature 2014; 505(7483):318–26.

12. Knopp A, Frahm C, Fidzinski P, Witte OW, Behr J. Loss of GABAergic neurons in the subiculum and its functional implications in temporal lobe epilepsy. Brain 2008; 131(Pt 6):1516–27.

13. Drexel M, Preidt AP, Kirchmair E, Sperk G. Parvalbumin interneurons and calretinin fibers arising from the thalamic nucleus reuniens degenerate in the subiculum after kainic acid-induced seizures. Neuroscience 2011; 189(1-2):316–29.

14. Drexel M, Romanov RA, Wood J, Weger S, Heilbronn R, Wulff P et al. Selective Silencing of Hippocampal Parvalbumin Interneurons Induces Development of Recurrent Spontaneous Limbic Seizures in Mice. J Neurosci 2017; 37(34):8166–79.

15. Dinocourt C, Petanjek Z, Freund TF, Ben-Ari Y, Esclapez M. Loss of interneurons innervating pyramidal cell dendrites and axon initial segments in the CA1 region of the hippocampus following pilocarpine-induced seizures. J Comp Neurol 2003; 459(4):407–25.

16. Drexel M, Rahimi S, Sperk G. Silencing of Hippocampal Somatostatin Interneurons Induces Recurrent Spontaneous Limbic Seizures in Mice. Neuroscience 2022; 487:155–65.

17. Klausberger T, Somogyi P. Neuronal diversity and temporal dynamics: the unity of hippocampal circuit operations. Science 2008; 321(5885):53–7.

18. Pelkey KA, Chittajallu R, Craig MT, Tricoire L, Wester JC, McBain CJ. Hippocampal GABAergic Inhibitory Interneurons. Physiol Rev 2017; 97(4):1619–747.

19. Kullander K, Topolnik L. Cortical disinhibitory circuits: cell types, connectivity and function. Trends Neurosci 2021; 44(8):643–57.

20. Lanerolle NC de, Gunel M, Sundaresan S, Shen MY, Brines ML, Spencer DD. Vasoactive intestinal polypeptide and its receptor changes in human temporal lobe epilepsy. Brain research 1995; 686(2):182–93.

21. Ko FJ, Chiang CH, Liu WJ, Chiang W. Somatostatin, substance P, prolactin and vasoactive intestinal peptide levels in serum and cerebrospinal fluid of children with seizure disorders. Gaoxiong Yi Xue Ke Xue Za Zhi 1991; 7(8):391–7.

22. Liang C, Zhang C-Q, Chen X, Wang L-K, Yue J, An N et al. Differential Expression Hallmarks of Interneurons in Different Types of Focal Cortical Dysplasia. J Mol Neurosci 2020; 70(5):796–805. Available from: URL: https://link.springer.com/article/10.1007/s12031-020-01492-0.

23. Hall S, Hunt M, Simon A, Cunnington LG, Carracedo LM, Schofield IS et al. Unbalanced Peptidergic Inhibition in Superficial Neocortex Underlies Spike and Wave Seizure Activity. J Neurosci 2015; 35(25):9302–14.

24. Henkel ND, Smail MA, Wu X, Enright HA, Fischer NO, Eby HM et al. Cellular, molecular, and therapeutic characterization of pilocarpine-induced temporal lobe epilepsy. Sci Rep 2021; 11(1):19102.

25. Wyeth M, Buckmaster PS. Lack of Hyperinhibition of Oriens Lacunosum-Moleculare Cells by Vasoactive Intestinal Peptide-Expressing Cells in a Model of Temporal Lobe Epilepsy. eNeuro 2021; 8(6).

26. David LS, Topolnik L. Target-specific alterations in the VIP inhibitory drive to hippocampal GABAergic cells after status epilepticus. Exp Neurol 2017; 292:102–12.

27. Cunha-Reis D, Caulino-Rocha A. VIP Modulation of Hippocampal Synaptic Plasticity: A Role for VIP Receptors as Therapeutic Targets in Cognitive Decline and Mesial Temporal Lobe Epilepsy. Front Cell Neurosci 2020; 14:153.

28. Kang Y-J, Clement EM, Park I-H, Greenfield LJ, Smith BN, Lee S-H. Vulnerability of cholecystokinin-expressing GABAergic interneurons in the unilateral intrahippocampal kainate mouse model of temporal lobe epilepsy. Exp Neurol 2021; 342:113724.

29. Acsády L, Arabadzisz D, Freund TF. Correlated morphological and neurochemical features identify different subsets of vasoactive intestinal polypeptide-immunoreactive interneurons in rat hippocampus. Neuroscience 1996; 73(2):299–315.

30. Yang K, Lei G, Jackson MF, Macdonald JF. The involvement of PACAP/VIP system in the synaptic transmission in the hippocampus. J Mol Neurosci 2010; 42(3):319–26.

31. Martin Shreeve S. Identification of G-proteins coupling to the vasoactive intestinal peptide receptor VPAC(1) using immunoaffinity chromatography: evidence for precoupling. Biochem Biophys Res Commun 2002; 290(4):1300–7.

32. Cunha-Reis D, Caulino-Rocha A, Correia-de-Sá P. VIPergic neuroprotection in epileptogenesis: challenges and opportunities. Pharmacol Res 2021; 164:105356.

33. Cunha-Reis D, Sebastião AM, Wirkner K, Illes P, Ribeiro JA. VIP enhances both pre- and postsynaptic GABAergic transmission to hippocampal interneurones leading to increased excitatory synaptic transmission to CA1 pyramidal cells. Br J Pharmacol 2004; 143(6):733–44.

34. Carvalho-Rosa JD, Cunha-Reis D. Endogenous VIP VPAC1 receptor activation during ictal and interictal-like activity induced in vitro by biccuculine and 0-Mg2+ modulates subsequent LTP expression in the rat hippocampus. Front Cell Neurosci 2019; 13.

35. Serpa A, Bento M, Caulino-Rocha A, Pawlak S, Cunha-Reis D. Opposing reduced VPAC1 and enhanced VPAC2 VIP receptors in the hippocampus of the Li2+-pilocarpine rat model of temporal lobe epilepsy. Neurochem Int 2022; 158:105383.

36. Lisgaras CP, Scharfman HE. Robust chronic convulsive seizures, high frequency oscillations, and human seizure onset patterns in an intrahippocampal kainic acid model in mice. Neurobiol Dis 2022; 166:105637.

37. González J, Cavelli M, Mondino A, Pascovich C, Castro-Zaballa S, Torterolo P et al. Decreased electrocortical temporal complexity distinguishes sleep from wakefulness. Sci Rep 2019; 9(1):18457.

38. Rusina E, Bernard C, Williamson A. The Kainic Acid Models of Temporal Lobe Epilepsy. eNeuro 2021; 8(2).

39. Murray AJ, Sauer J-F, Riedel G, McClure C, Ansel L, Cheyne L et al. Parvalbumin-positive CA1 interneurons are required for spatial working but not for reference memory. Nat Neurosci 2011; 14(3):297–9.

40. Mietzsch M, Broecker F, Reinhardt A, Seeberger PH, Heilbronn R. Differential adeno-associated virus serotype-specific interaction patterns with synthetic heparins and other glycans. J Virol 2014; 88(5):2991–3003.

41. Tasan RO, Nguyen NK, Weger S, Sartori SB, Singewald N, Heilbronn R et al. The central and basolateral amygdala are critical sites of neuropeptide Y/Y2 receptor-mediated regulation of anxiety and depression. J Neurosci 2010; 30(18):6282–90.

42. Auer T, Schreppel P, Erker T, Schwarzer C. Functional characterization of novel bumetanide derivatives for epilepsy treatment. Neuropharmacology 2020; 162:107754.

43. Sharma S, Puttachary S, Thippeswamy A, Kanthasamy AG, Thippeswamy T. Status Epilepticus: Behavioral and Electroencephalography Seizure Correlates in Kainate Experimental Models. Front. Neurol. 2018; 9.

44. Zijlmans M, Worrell GA, Dümpelmann M, Stieglitz T, Barborica A, Heers M et al. How to record high-frequency oscillations in epilepsy: A practical guideline. Epilepsia 2017; 58(8):1305–15.

45. Lisgaras CP, Scharfman HE. High-frequency oscillations (250-500 Hz) in animal models of Alzheimer's disease and two animal models of epilepsy. Epilepsia 2023; 64(1):231–46.

46. Zhou G, Noto T, Sharma A, Yang Q, González Otárula KA, Tate M et al. HFOApp: A MATLAB Graphical User Interface for High-Frequency Oscillation Marking. eNeuro 2021; 8(5).

47. Staba RJ, Wilson CL, Bragin A, Fried I, Engel J. Quantitative analysis of high-frequency oscillations (80-500 Hz) recorded in human epileptic hippocampus and entorhinal cortex. J Neurophysiol 2002; 88(4):1743–52.

48. Navarrete M, Alvarado-Rojas C, van Quyen M, Valderrama M. RIPPLELAB: A Comprehensive Application for the Detection, Analysis and Classification of High Frequency Oscillations in Electroencephalographic Signals. PLoS ONE 2016; 11(6):e0158276.

49. Salami P, Lévesque M, Benini R, Behr C, Gotman J, Avoli M. Dynamics of interictal spikes and high-frequency oscillations during epileptogenesis in temporal lobe epilepsy. Neurobiol Dis 2014; 67:97–106.

50. Matsumoto A, Brinkmann BH, Matthew Stead S, Matsumoto J, Kucewicz MT, Marsh WR et al. Pathological and physiological high-frequency oscillations in focal human epilepsy. J Neurophysiol 2013; 110(8):1958–64.

S1 Table. The number, duration and amplitude of isolated FRs remained consistent before and after vector injection, during both the light and dark phases.

		Before						After						Ratio					
		GFP		**TeLC**		**Difference**		**GFP**		**TeLC**		**Difference**		**GFP**		**TeLC**		**Difference**	
		Median	Range	Median	Range	p value	Sig?	Median	Range	Median	Range	p value	Sig?	Median	Range	Median	Range	p value	Sig?
Number	**Light**	3.083	13.67	2.25	7.50	0.42	No	2.41	5.33	1.58	17.50	0.70	No	-0.23	1.14	-0.04	1.71	0.27	No
	Dark	2.50	10.00	2.16	6.03	0.81	No	0.50	10.83	0.75	12.83	0.55	No	-0.67	1.66	-0.44	1.85	0.58	No
Duration	**Light**	16.16	14.02	19.17	8.90	0.19	No	15.34	9.37	14.09	9.81	0.95	No	-0.02	1.08	-0.14	0.44	0.79	No
	Dark	14.52	16.88	15.81	13.53	0.87	No	13.00	6.23	14.75	5.65	0.75	No	-0.05	1.07	-0.08	1.04	0.81	No
Amplitude	**Light**	7.04	7.64	11.28	9.99	0.10	No	5.39	2.78	5.04	2.21	0.95	No	-0.18	1.04	-0.34	0.48	0.32	No
	Dark	5.68	15.03	6.66	10.52	0.57	No	5.21	1.91	5.04	1.97	0.75	No	--0.10	0.97	-0.19	0.96	0.73	No

Figure legends

Fig 1. Silencing of subicular VIP-INs does not induce seizures in healthy mice.

(A) The study protocol and the coordinates for intrahippocampal AAV-TeLC (*n*=5) and AAV-GFP (*n*=5) injections in non-epileptic mice, followed by long-term telemetric EEG recordings.

(B) Representative 1 min EEG-trace obtained 14 days after AAV-TeLC injection. No seizures were observed during the 50 days recording period.

(C) The rate of GFP expression in cells. At the injection site, 46.67% (41.18% to 90%) of the VIP-INs expressed GFP (101 cells out of 169 cells), while 95.84% (82.35% to 100%) of the GFP-expressing interneurons also co-expressed VIP (101 cells out of 108 cells; *n*=4 mice from GFP group, *n*=4 mice from TeLC group).

Fig 2. Silencing subicular VIP-INs in epileptic mice alleviates seizures.

(A) The study protocol and the coordinates and for Injection of IH-KA (200 ng), AAV-TeLC (*n*=8), and AAV-GFP (*n*=8). The frequency and duration of seizures were evaluated on Day one (SE), the six days following KA injection (Day 2 to Day 7), as well as on the six days, commencing two weeks after vector injection (Day 22 to Day 27).

(B) Representative seizure recorded 3 days after IH-KA injection. In general, seizures are preceded by a series of numerous epileptiform spikes and were detected based on continuous activity lasting at least 10 seconds with an amplitude that was at least twice that of the baseline, accompanied by postictal depression.

(C) During SE, the median (range) number of seizures was 10 (1 to 19) and 8.5 (1 to 14) for the GFP (*n*=8) and TeLC (*n*=8) groups, respectively, and there was no significant difference between the groups (Two-tailed Mann-Whitney test; $p = 0.625$).

(D) Before vector injection, the median (range) number of seizures was 1.50 (1 to 12) and 4.50 (2 to 13) for the GFP (*n*=8) and TeLC (*n*=8) groups, respectively. No significant difference between the groups was observed (Two-way ANOVA test; $F = 0.701$, $p = 0.417$).

(E) After vector injection, the median (range) number of seizures was 7 (0 to 14) in the GFP group (*n*=8) and 3 (0 to 7) for the TeLC group (*n*=8). A significant difference was found between the groups (Two-way ANOVA test; $F = 6.749$, $p = 0.021$).

(F) According to two-way ANOVA test, groups showed a significant different trend in seizure development ($F = 7.548$, $p = 0.015$ for interaction of time and the vector injection). A post-hoc Šídák comparison indicated the significant difference in the number of seizures after vector injection ($p = 0.041$).

(G) The median (range) seizure ratio was 0.55 (-1.00 to 0.86) for the GFP group (*n*=8) and -0.33 (-1.00 to 0.42) for the TeLC group (*n*=8). A significant difference was reported according to two-tailed Mann-Whitney test ($p = 0.022$).

(H) According to two-way ANOVA test, the reduction in the number of seizures was more prominent during the light phase ($p = 0.044$, post-hoc Šídák test) in comparison to the dark phase ($p = 0.369$, post-hoc Šídák test)

(I) During SE, the median (range) cumulative duration of seizures was 314.1 s (10.34 s to 1098 s) for the GFP group (*n*=8) and 266.10 s (17 s to 703 s) for the TeLC group (*n*=8). No significant difference between the groups according to two-tailed Mann-Whitney test (p = 0.645).

(J) The median (range) time spent in seizure (cumulative duration) prior to vector injection was 48.81 s (10 s to 517 s) for GFP mice (*n*=8) and 168.8 s (87.36 s to 210.70 s) for TeLC mice (*n*=8), respectively. No significant difference between the groups was observed according to two-way ANOVA test ($F = 0.700$, $p = 0.416$).

(K) After vector injection, the median (range) cumulative duration of seizures was 285.4 s (0 to 499.4 s) and 85.15 s (0.0 to 264.4 s) for the GFP group (n=8) and TeLC group (n=8), respectively. A significant difference was found between the groups according to two-way ANOVA test (F = 7.517, p = 0.015).

(L) According to two-way ANOVA test, over time, there was a significant difference in time spent in seizures between groups (F = 6.204, p = 0.025 for interaction of time and the vector injection). A post-hoc Šídák comparison indicated the significant difference in the cumulative duration of seizures after vector injection (p = 0.043).

(M) The median (range) of seizure duration ratio was 0.66 (-1.0 to 0.96) for GFP mice (n=8) and -0.36 (-1.0 to 0.34) for TeLC mice (n=8). A significant difference was reported according to two-tailed Mann-Whitney test (p = 0.027).

(N) According to two-way ANOVA test, the decrease in the cumulative duration of seizures was more pronounced during the light phase (p = 0.042, post-hoc Šídák test) as compared to the dark phase (p = 0.323, post-hoc Šídák test).

Fig 3. Activating VIP-INs in acute seizure model results in increased seizure frequency.

(A) The study protocol and the coordinates and for Injection of AAV-hM3D(Gq, *n*=15) and IH-KA (70 ng). The animals were blindly divided into two groups, NaCl (*n*=6) and CNO (*n*=9), receiving i.p. injection of NaCl and CNO at Day 10, respectively. The *i.p.* injection was administered 30 minutes prior to the IH-KA injection.

(B) The number of seizures for each individual animal in the first 60 minutes after IH-KA injection (bin of 10 minutes).

(C) After IH-KA injection, animals in NaCl (*n*=6) and CNO (*n*=9) group developed seizures. A significant difference was found between the groups (Two-way ANOVA test; $F = 5.353$, $p = 0.037$).

(D) The median (range) number of seizures in the NaCl group was 2 (1 to 4), while the value was 5 (2 to 7) for the CNO group. A significant difference was reported according to two-tailed Mann-Whitney test ($p = 0.034$).

(E) The median (range) cumulative duration of seizures for the NaCl group was 76.02 s (33.08 s to 150.50 s) and 138.70 s (51.89 s to 225.0 s) for the CNO group. There were no significant differences between the groups, despite a strong trend ($p = 0.087$, according to two-tailed Mann-Whitney test).

Fig 4. How manipulating subicular VIP-INs can alter seizure occurrence

(A) In the absence of manipulation (left), VIP-BC directly innervate PCs, while IS type II and III primarily target other interneurons, leading to disinhibition of PCs. However, when both groups of VIP-INs were silenced (right), we observed a predominant role of IS type II and III, which resulted in the absence of seizures.

(B) In the epileptic condition, silencing VIP-INs may have an opposite effect (left). While silencing VIP-BCs can exacerbate seizures, silencing IS type II and III indirectly increases the final inhibition of PCs. Our experimental results support a prominent role of IS type II and III interneurons over VIP-BCs in the course of epilepsy. Activation of VIP-INs (right) can also have an opposite effect. Activation of VIP-BCs can decrease seizure occurrence, but activating IS type II and III can enhance seizure development. However, the outcome of the experiment highlights the greater impact of IS type II and III compared to VIP-BCs in the development of seizures.

S1 Fig. Bilateral silencing of subicular VIP-INs does not prompt epileptiform activity.

(A) The study protocol and the coordinates for bilateral intrahippocampal AAV-TeLC (*n*=4) and AAV-GFP (*n*=4) injections in non-epileptic mice, followed by telemetric long-term LFP recording from dorsal CA1. No seizures were observed during the 21 days recording period.

(B) Representative example of detected epileptiform spikes in 1 min EEG-traces obtained 18 days after AAV-TeLC injection. The algorithm employs a set of features, including duration (10 to 80 ms) and amplitude (above a predefined threshold) to detect interictal spikes with epileptiform characteristics. A minimum peak distance of 150 ms between identified spikes was required. Detected spikes were then visually confirmed.

(C) The median (range) cumulative number of epileptiform spikes (for the entire 24-hour assessment) was 148 (3 to 1687) and 1500 (24 to 4723) for GFP (*n*=4) and TeLC animals (*n*=4). There was no significant difference between the groups according to two-tailed Mann-Whitney test (p=0.343).

(D) The median (range) number of spike trains was 0.0 (0.0 to 37) and 13.50 (0.0 to 31) for GFP (*n*=4) and TeLC animals (*n*=4), respectively, and there was no significant difference between the groups according to two-tailed Mann-Whitney test ($p > 0.99$).

S2 Fig. No difference was observed in severity of SE between groups.

(A) The study protocol and the coordinates and for Injection of IH-KA (*n*=16). The animals were blindly divided into two groups, GFP (*n*=8) and TeLC (*n*=8), receiving AAV-GFP or AAV-TeLC after 7 days, respectively.

(B) Representative example of SE in first 24 hours after IH-KA injection. Postictal depression is not always visible during SE.

(C) During SE, the median (range) hourly number of epileptiform spikes was 3149 (1786 to 4071) and 3767 (206.8 to 4633) for GFP (*n*=8) and TeLC (*n*=8) groups, respectively. No significant difference was found between the groups according to two-way ANOVA test ($F = 0.252$, $p = 0.623$).

(D) The median (range) number of epileptiform spikes in the GFP group (*n*=8) was 54511 (32651 to 153106) and 68674 (33018 to 153892) for TeLC mice (*n*=8). There was no significant difference between the groups according to two-tailed Mann-Whitney test ($p = 0.878$).

(E) During SE, the median (range) hourly number of spike trains was 283 (110.4 to 401.6) and 324.2 (6.62 to 471.90) for GFP (*n*=8) and TeLC (*n*=8) groups, respectively. No significant difference was found between the groups according to two-way ANOVA test ($F = 0.058$, $p = 0.813$).

(F) The median (range) number of spike trains was 3519 (1993 to 18226) for the GFP group (*n*=8) and 6439 (1996 to 15306) for the TeLC group (*n*=8). There was no significant difference between the groups according to two-tailed Mann-Whitney test ($p = 0.645$).

S3 Fig. Circadian variation in seizure ratio among the individual animals.

(A) For each animal, the seizure ratio was calculated by comparing the number of seizures after vector injection (six days, starting from day 22) to the number of seizures before vector injection (six days, excluding SE).

(B) Each cycle displays a single animal from either the GFP (n = 8) or TeLC group (n = 8), with each rectangle indicating the seizure ratio in one hour during the 24-hour day.

S4 Fig. Isolated FRs recorded outside of the subiculum do not change in the same manner as seizures

(A) Fast ripples were detected, and their features were evaluated from Day 2 to Day 7 (a selected time period before vector injection) and again over Day 22 to Day 27 (14 days after vector injection). For each mouse, two 10 minutes periods (one during light phase, one during the dark phase) were sampled for each day.

(B) A representative 100 ms example of raw EEG signals (top trace), and filtered traces in ripple frequency band (80-250 Hz; middle trace) and fast ripple frequency band (250-500 Hz; bottom trace). The FRs that were detected by the automated method were further evaluated visually along with the time-freqeuncy power spectrum. False detections caused by artifacts or sharp events and overlapping fast ripples with ripples were excluded.

(C) Before vector injection, the median (range) number of isolated FRs per 10-minute bin was 3.08 (0.83 to 14.50) for the GFP group (*n*=8) and 2.25 (0.50 to 8.00) for the TeLC group (*n*=8) during the light phase. After vector injection, the median (range) number of isolated FR in each 10-minute bin was 2.41 (0.00 to 5.33) for the GFP group and 1.58 (0.33 to 17.83) for the TeLC group. No significant difference between the groups was observed (Two-way ANOVA test; F = 1.696, p = 0.213). The median (range) of incidence ratio of isolated FRs during the light phase was 0.66 (-1.0 to 0.96) for GFP mice (*n*=8) and -0.36 (-1.00 to 0.34) for TeLC mice (*n*=8). No significant difference was reported (Two-tailed Mann-Whitney test; p = 0.278).

(D) The median (range) value for the average duration of isolated FRs per 10-minute bin was 16.16 ms (13.83 ms to 27.85 ms) for the GFP group (*n*=8) and 19.17 ms (16.07 ms to 24.98 ms) for the TeLC group (*n*=8) during the light phase in the six days before vector injection. After injection, the median (range) value for the average duration of isolated FRs in each 10-minute bin was 15.34 ms (10.00 ms to 19.37 ms) for the GFP group (*n*=7, one mouse had no isolated FRs) and 14.09 ms (12.75 ms to 22.56 ms) for the TeLC group (*n*=8). Data were analyzed by fitting a mixed model and no difference was observed between groups (F = 1.597, p = 0.692). The median (range) duration ratio of isolated FRs during the light phase was -0.02 (-1.00 to 0.08) for GFP mice (*n*=8) and -0.14 (-0.27 to 0.16) for TeLC mice (*n*=8). No significant difference was reported (Two-tailed Mann-Whitney test; p = 0.798).

(E) Before vector injection, the median (range) value for the average amplitude of isolated FRs per 10-minute bin was 7.04 μV (5.21 μV to 12.86 μV) for the GFP group (*n*=8) and 11.28 μV (5.61 μV to 15.61 μV) for the TeLC group (*n*=8) during the light phase. After vector injection, the median (range) value for the average amplitude of isolated FRs in each 10-minute bin was 5.39 μV (4.41 μV to 7.20 μV) for the GFP group (*n*=7, one mouse had no isolated FRs) and 5.04 μV (4.62 μV to 6.84 μV) for the TeLC group (*n*=8). Data were analyzed by fitting a mixed model and no difference was observed between groups (F = 3.686, p = 0.065). The median (range)

amplitude ratio of isolated FRs during the light phase was -0.18 (-1.00 to 0.04) for GFP mice (*n*=8) and -0.34 (-0.51 to -0.03) for TeLC mice (*n*=8). No significant difference was reported (Two-tailed Mann-Whitney test; $p = 0.328$).

(F) During the dark phase, before vector injection, the median (range) number of isolated FRs per 10-minute bin was 2.50 (0.33 to 10.33) for the GFP group (*n*=8) and 2.16 (0.16 to 6.20) for the TeLC group (*n*=8). After vector injection, the median (range) number of isolated FR in each 10-minute bin was 0.50 (0.00 to 10.83) for the GFP group and 0.75 (0.00 to 12.83) for the TeLC group. No significant difference between the groups was observed (Two-way ANOVA test; $F = 0.294$, $p = 0.595$). The median (range) incidence ratio of isolated FRs during the dark phase was -0.67 (-1.0 to 0.66) for GFP mice (*n*=8) and -0.44 (-1.00 to 0.85) for TeLC mice (*n*=8). No significant difference was reported (Two-tailed Mann-Whitney test; $p = 0.586$).

(G) Before vector injection, the median (range) value for the average duration of isolated FRs per 10-minute bin was 14.52 ms (11.37 ms to 28.25 ms) for the GFP group (*n*=8) and 15.81 ms (11.00 ms to 24.53 ms) for the TeLC group (*n*=8) during the dark phase. After vector injection, the median (range) value for the average duration of isolated FRs in each 10-minute bin was 13.00 ms (12.33 ms to 18.56 ms) for the GFP group (*n*=5, three animals had no isolated FRs) and 14.75 ms (11.84 ms to 17.49 ms) for the TeLC group (*n*=7, one mouse had no isolated FRs). Data were analyzed by fitting a mixed model and no difference was observed between groups ($F = 2.015$, $p = 0.186$). The median (range) duration ratio of isolated FRs during the dark phase was -0.05 (-1.00 to 0.07) for GFP mice (*n*=8) and -0.08 (-1.00 to 0.04) for TeLC mice (*n*=8). No significant difference was reported (Two-tailed Mann-Whitney test; $p = 0.811$).

(H) The median (range) value for the average amplitude of isolated FRs per 10-minute bin was 5.67 μV (4.92 μV to 19.96 μV) for the GFP group (*n*=8) and 6.66 μV (4.30 μV to 14.82 μV) for the TeLC group (*n*=8) during the dark phase before vector injection. After vector injection, the median (range) value for the average amplitude of isolated FRs in each 10-minute bin was 5.21 μV (4.71 μV to 6.62 μV) for the GFP group (*n*=5, three animals had no isolated FRs) and 5.04 μV (4.40 μV to 6.37 μV) for the TeLC group (*n*=7, one mouse had no isolated FRs). Data were analyzed by fitting a mixed model and no difference was observed between groups ($F = 0.913$, $p = 0.361$). The median (range) amplitude ratio of isolated FRs during the dark phase was -0.10 (-1.00 to -0.02) for GFP mice (*n*=8) and -0.19 (-1.00 to -0.03) for TeLC mice (*n*=8). No significant difference was reported (Two-tailed Mann-Whitney test ($p = 0.733$).

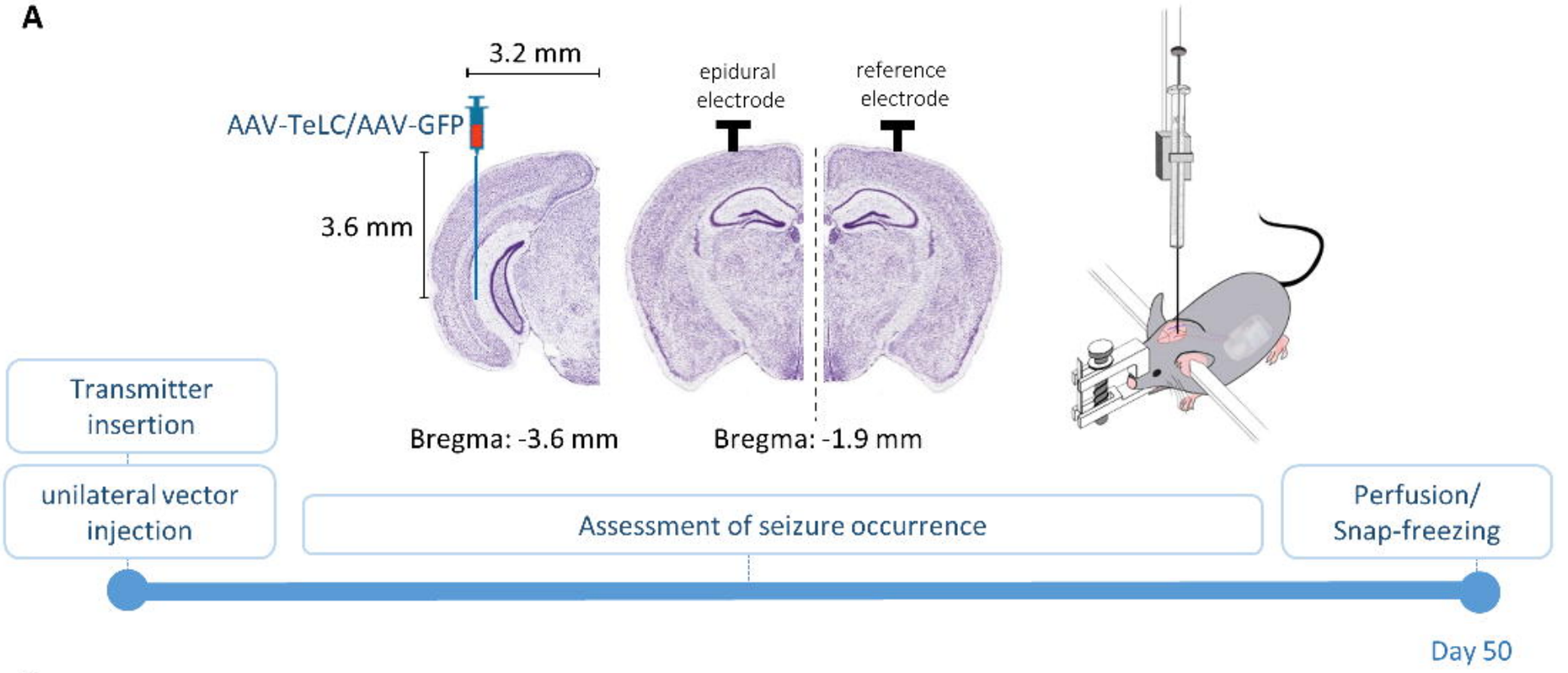
A
3.2 mm
AAV-TeLC/AAV-GFP
3.6 mm
epidural electrode
reference electrode
Bregma: -3.6 mm
Bregma: -1.9 mm
Transmitter insertion
unilateral vector injection
Assessment of seizure occurrence
Perfusion/ Snap-freezing
Day 50

B
0.5 mV
5 s

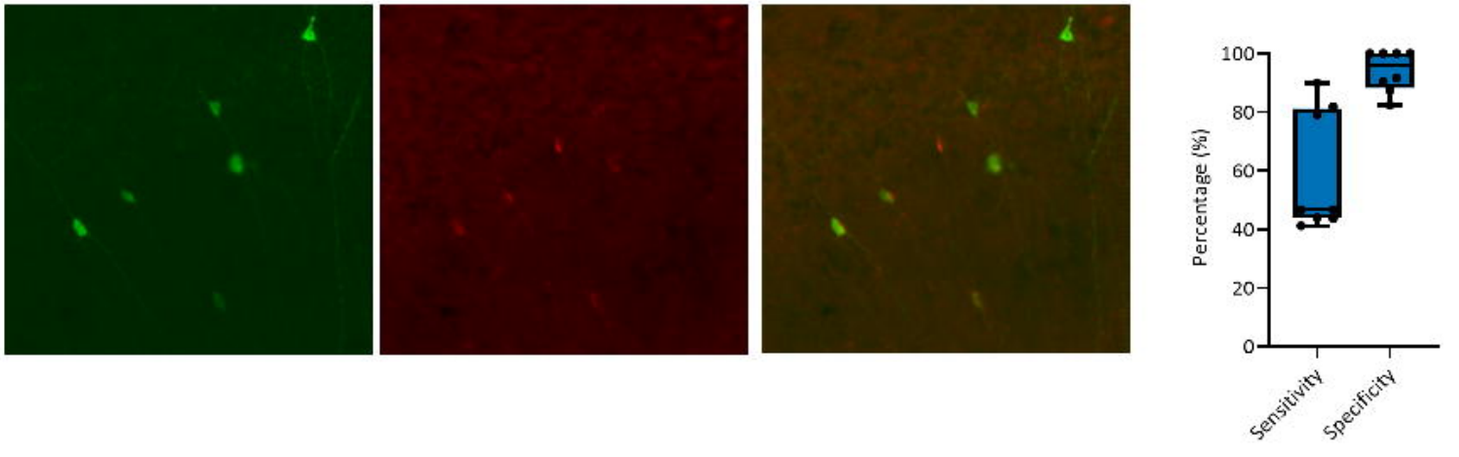
C
Percentage (%)
100
80
60
40
20
0
Sensitivity
Specificity

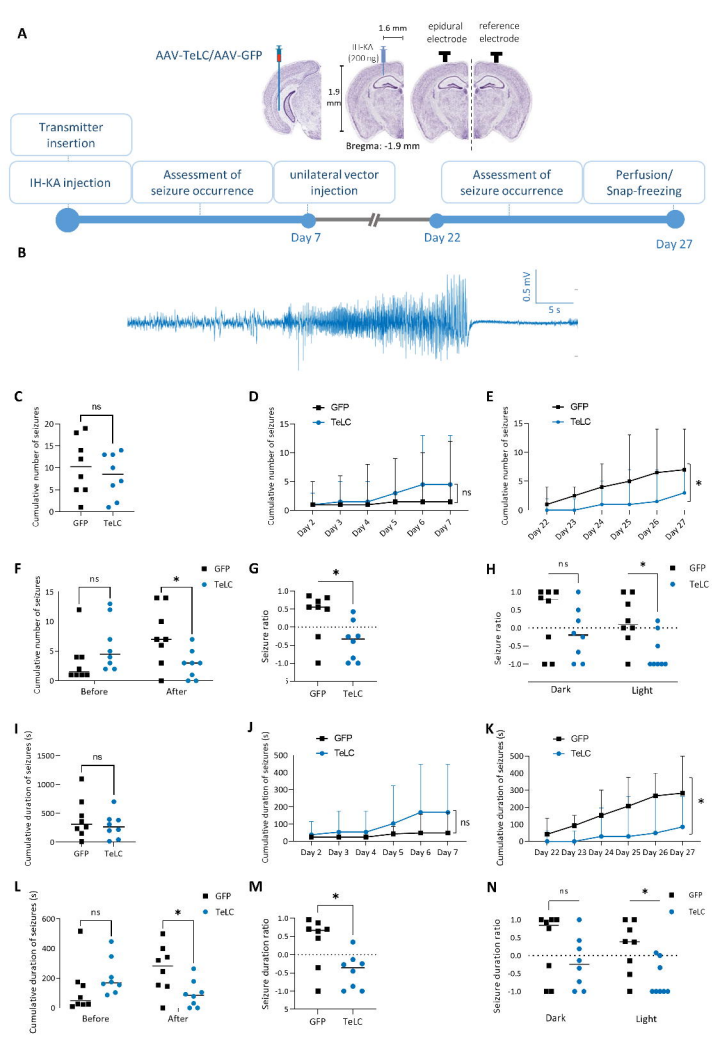
A
AAV-TeLC/AAV-GFP
1.6 mm
IH-KA (200 ng)
1.9 mm
epidural electrode
reference electrode
Bregma: -1.9 mm
Transmitter insertion
IH-KA injection
Assessment of seizure occurrence
unilateral vector injection
Assessment of seizure occurrence
Perfusion/ Snap-freezing
Day 7
Day 22
Day 27
B
0.5 mV
5 s
C
ns
Cumulative number of seizures
GFP
TeLC
D
GFP
TeLC
Cumulative number of seizures
ns
Day 2
Day 3
Day 4
Day 5
Day 6
Day 7
E
GFP
TeLC
Cumulative number of seizures
*
Day 22
Day 23
Day 24
Day 25
Day 26
Day 27
F
GFP
TeLC
Cumulative number of seizures
ns
*
Before
After
G
*
Seizure ratio
GFP
TeLC
H
GFP
TeLC
ns
*
Seizure ratio
Dark
Light
I
ns
Cumulative duration of seizures (s)
GFP
TeLC
J
GFP
TeLC
Cumulative duration of seizures (s)
ns
Day 2
Day 3
Day 4
Day 5
Day 6
Day 7
K
GFP
TeLC
Cumulative duration of seizures (s)
*
Day 22
Day 23
Day 24
Day 25
Day 26
Day 27
L
GFP
TeLC
Cumulative duration of seizures (s)
ns
*
Before
After
M
*
Seizure duration ratio
GFP
TeLC
N
GFP
TeLC
ns
*
Seizure duration ratio
Dark
Light

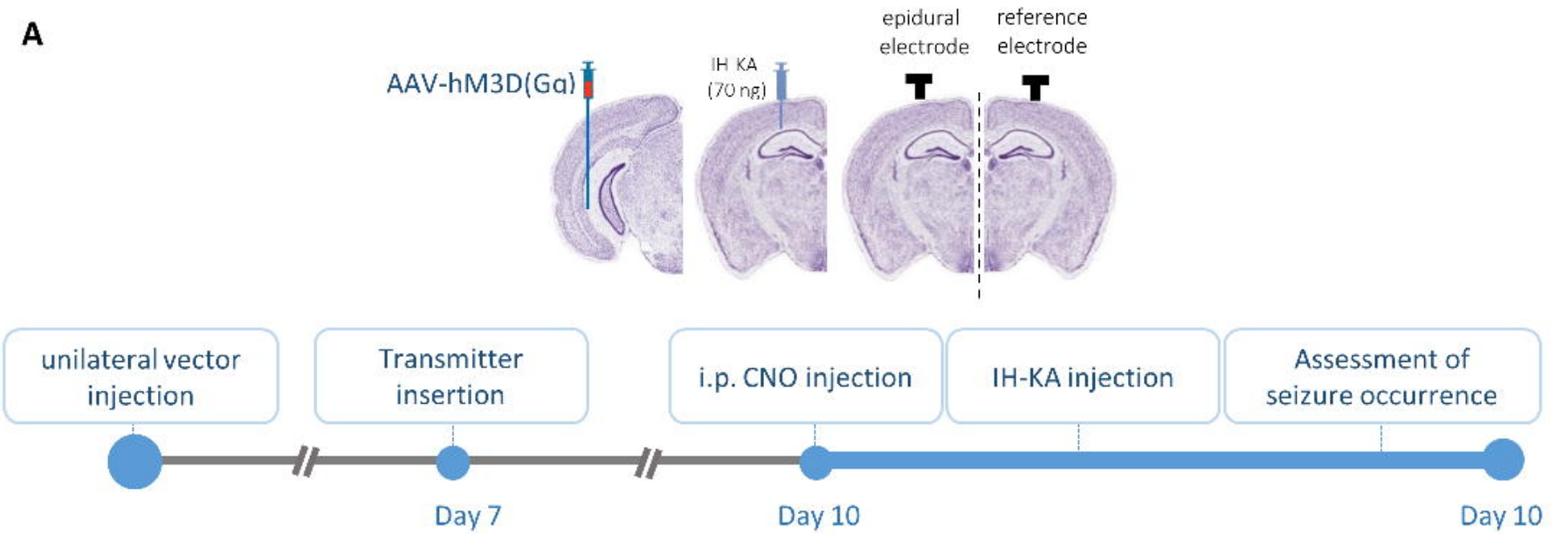
A
AAV-hM3D(Gq)
IH KA
(70 ng)
epidural
electrode
reference
electrode
unilateral vector
injection
Transmitter
insertion
i.p. CNO injection
IH-KA injection
Assessment of
seizure occurrence
Day 7
Day 10
Day 10

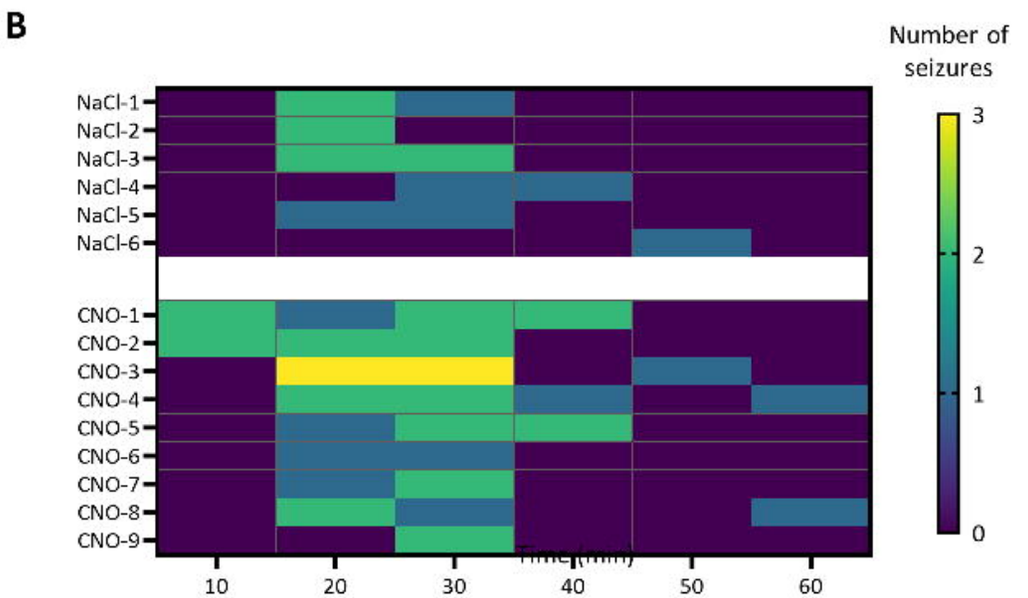
B
Number of
seizures
NaCl-1
NaCl-2
NaCl-3
NaCl-4
NaCl-5
NaCl-6
CNO-1
CNO-2
CNO-3
CNO-4
CNO-5
CNO-6
CNO-7
CNO-8
CNO-9
Time (min)
10
20
30
40
50
60
3
2
1
0

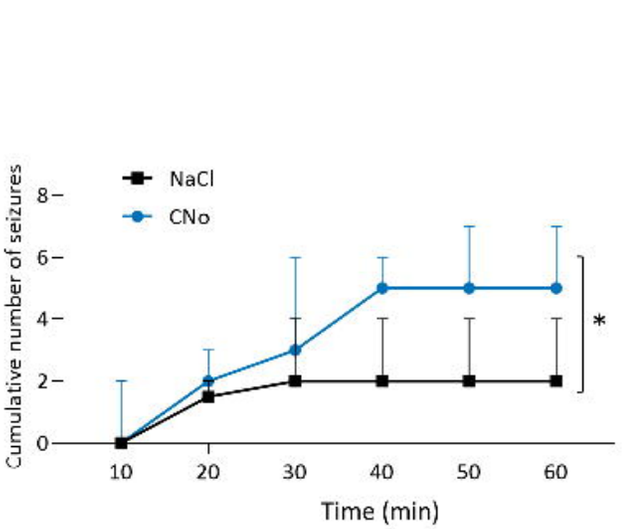
C
NaCl
CNo
Cumulative number of seizures
Time (min)
0
2
4
6
8
10
20
30
40
50
60
*

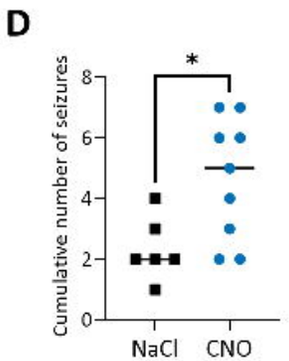
D
Cumulative number of seizures
0
2
4
6
8
*
NaCl
CNO

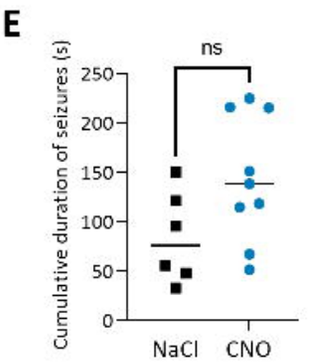
E
Cumulative duration of seizures (s)
0
50
100
150
200
250
ns
NaCl
CNO

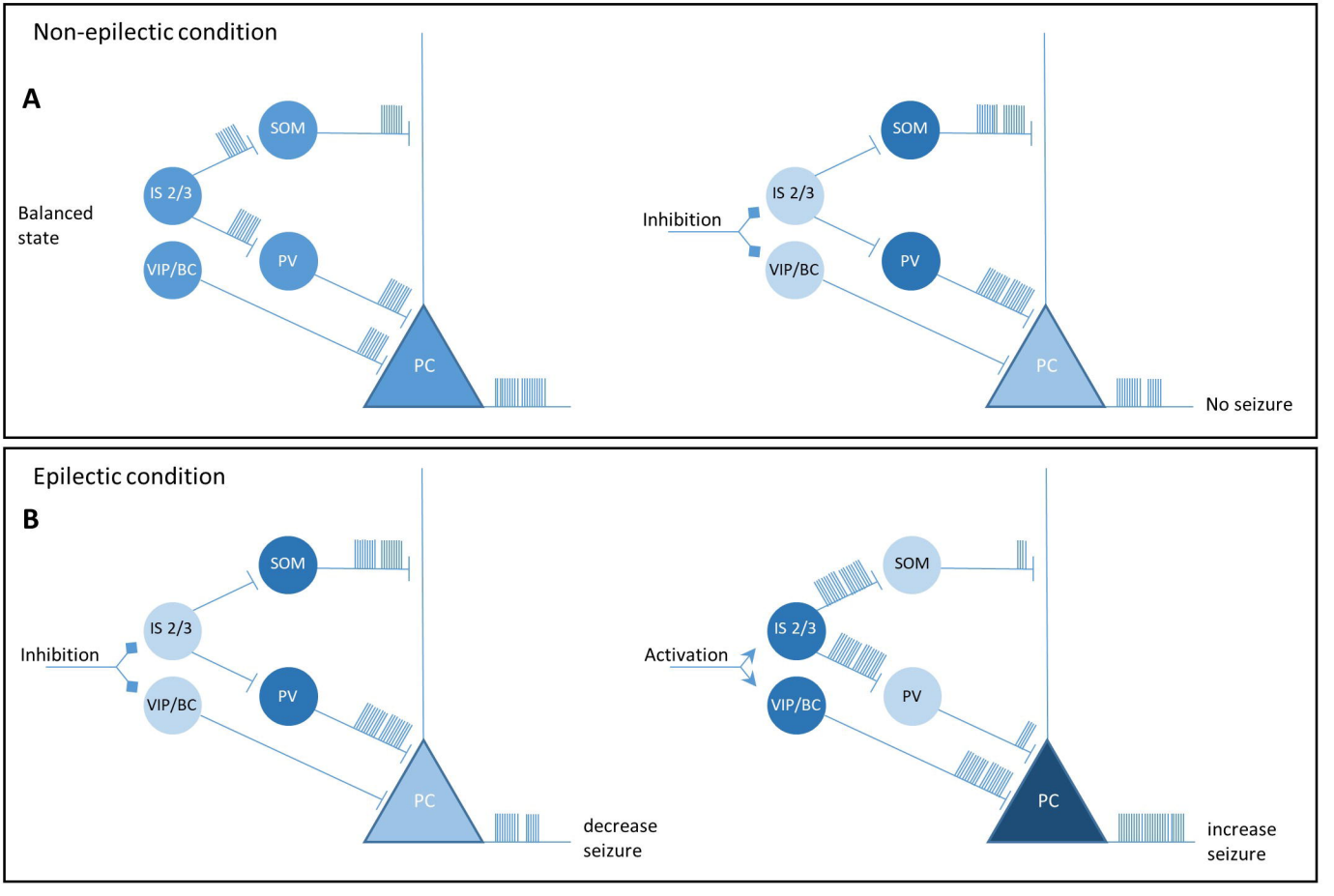
Non-epilectic condition
A
Balanced state
IS 2/3
SOM
VIP/BC
PV
PC
Inhibition
IS 2/3
SOM
VIP/BC
PV
PC
No seizure
Epilectic condition
B
Inhibition
IS 2/3
SOM
VIP/BC
PV
PC
decrease seizure
Activation
IS 2/3
SOM
VIP/BC
PV
PC
increase seizure